



HAL
open science

A Stochastic Geometry Based Approach to Tractable 5G RNPO with a New H-LOS Model

Yassine Hmamouche, Mustapha Benjillali, Samir Saoudi

► **To cite this version:**

Yassine Hmamouche, Mustapha Benjillali, Samir Saoudi. A Stochastic Geometry Based Approach to Tractable 5G RNPO with a New H-LOS Model. WCNC 2019: IEEE Wireless Communications and Networking Conference, Apr 2019, Marrakech, Morocco. 10.1109/WCNC.2019.8885422 . hal-02067720

HAL Id: hal-02067720

<https://imt-atlantique.hal.science/hal-02067720>

Submitted on 14 Mar 2019

HAL is a multi-disciplinary open access archive for the deposit and dissemination of scientific research documents, whether they are published or not. The documents may come from teaching and research institutions in France or abroad, or from public or private research centers.

L'archive ouverte pluridisciplinaire **HAL**, est destinée au dépôt et à la diffusion de documents scientifiques de niveau recherche, publiés ou non, émanant des établissements d'enseignement et de recherche français ou étrangers, des laboratoires publics ou privés.

A Stochastic Geometry Based Approach to Tractable 5G RNPO with a New H -LOS Model

Yassine Hmamouche^{1,2}, Mustapha Benjillali², and Samir Saoudi¹

¹ IMT Atlantique, Lab-STICC, UBL, 29238 Brest, France

Emails: {yassine.hmamouche; samir.saoudi}@imt-atlantique.fr

² Communication Systems Department, INPT, Rabat, Morocco

Email: benjillali@ieee.org

Abstract—We consider a 3D cellular network in which generalized shadowing and radio network planning and optimisation (RNPO) parameters (e.g., antenna height, antenna tilt/azimuth, power biasing...) are incorporated into the cell-selection model. Using tools from stochastic geometry (SG), we derive an equivalent 2D network in which no shadowing and RNPO parameters are considered. Next, we derive coverage probability for a tractable case-study network, and the regimes where coverage probability is maximized in addition to the interference-limited one are investigated. An intermediary result is a closed-form expression generator encompassing the Q -function based-expression in [1]. Numerical results confirm the accuracy of our approximations.

I. INTRODUCTION

With the ongoing proliferation of data-hungry devices and applications, data traffic volumes in the coming years are expected to be multi-fold higher compared to today's levels. One way to tackle this challenge is by deploying ultra-dense networks (UDNs) [2]. However, densification will result in large coverage overlap areas, which increases the risk of other-cell interference and then reduces the network performance and system capacity. Consequently, environment characteristics such as shadowing, and RNPO parameters such as antenna height [3], antenna tilt/azimuth angle [4]- [6] and transmit power biasing [7] are strongly required for the analysis of UDNs performance since they affect directly the probability of line-of-sight (LOS) and non-line-of-sight (NLOS) connections and then cells overlapping.

Due to its tractability and ability to capture spatial averages, SG has emerged as a potential mathematical tool for modeling cellular networks [1], [3]- [7]. In fact, by considering a standard path-loss model and ignoring shadowing and any RNPO parameter effect, the seminal work in [1] provides comprehensive understanding about the behavior of UDNs performance. An important outcome is the signal-to-interference-plus-noise ratio (SINR) invariance property, which states that the SINR increases almost linearly with base station (BS) density to the point where noise becomes negligible; after which SINR remains stable and independent from BS density. However, using standard path-loss model and ignoring RNPO parameters in more realistic scenarios has raised some limitations [8],

calling for an imperative revisitation of the model. Authors of [9] proved that the SINR invariance property is no longer valid when using the dual-slope path-loss model. A similar effect is reported in [3] for elevated BSs, and in [4] for a network using non-directional antennas.

The motivation behind this paper is then to find a tractable manner to study UDNs performance when incorporating generalized shadowing and RNPO parameters into the cell-selection model. Using tools from SG, we first *i)* develop a 3D-2D *network equivalence* where a 3D network with shadowing and RNPO parameters is *stochastically equivalent* to a 2D network in which they are not considered. Next, for mathematical convenience, *ii)* we focus our analysis on a tractable case-study in which shadowing and RNPO parameters are captured via aggregated parameters related with LOS and NLOS connections. *iii)* The coverage probability is then computed confirming that our expression is general enough to accommodate several previous expressions. Next, *iv)* we investigate the scaling law of the BS density that maximizes network performance as well as the coverage probability in the interference-limited regime.

The following notation will be used throughout the paper. $\mathbb{P}\{\cdot\}$ and $\mathbb{E}\{\cdot\}$ stand for the probability and expectation measure. $\mathbb{L}_X(s) = \mathbb{E}\{e^{-sX}\}$ is the Laplace transform of a random variable X evaluated at s . We define for any reals $m, x \in \mathbb{R}$, $F_m(x) = {}_2F_1(1, m; m+1; -x)$ where ${}_2F_1(\cdot, \cdot; \cdot; z)$ is the Gauss hypergeometric function. $g^{-1}(\cdot)$ is the inverse function of a function $g(\cdot)$.

II. SYSTEM MODEL AND THE PATH LOSS PROCESS WITH SHADOWING AND RNPO PARAMETERS (PLPSR)

A. System Model

We consider a downlink cellular network, in which BSs are scattered randomly according to a homogeneous PPP $\Phi_b \in \mathbb{R}^3$ with density λ_b . We assume that each BS is equipped with directional antennas, has at least one connected user and transmits with a fixed power P_{tx} . Denote σ^2 the variance of the additive noise and $\text{SNR} = P_{tx}/\sigma^2$. We consider a realization of RNPO parameters of interest: BS antenna elevation height parametrized by a random variable ξ_{x_h} , electrical/mechanical antenna tilt angle by ξ_{x_t} , antenna azimuth angle by ξ_{x_a} and range expansion (RE) bias by ξ_{x_b} . For each BS $x \in \Phi_b$,

This work is funded by a research grant from PRACOM and the Regional Council of Brittany, France.

we add independent¹ marks $(h_x, \chi_x, \xi_x, \alpha_x, T_x)$, where for the link between x and the typical user located at O , h_x denote the small scale fading assumed to be exponentially distributed with unit mean, χ_x is the shadowing effect assumed to be arbitrarily distributed, α_x is the path-loss exponent, T_x is the SINR threshold of x , and ξ_x is the vector $\xi_x = (\xi_{x_h}, \xi_{x_t}, \xi_{x_a}, \xi_{x_b})$ of RNPO parameters, such as the received power at O from the BS $x \in \Phi_b$ is

$$P_{rx} = \frac{\chi_x h_x P_{tx}}{(\Psi(r_x; \alpha_x; \xi_x))^{\alpha_x}}, \quad (1)$$

where r_x is the horizontal distance between x and O , and $\Psi(\cdot)$ is a generalized function to capture RNPO parameters combined with the path-loss function. If there is such a function, it is reasonable to require of it the following properties: (i) monotonically increasing such as $\Psi(0; \cdot; \xi_{x_h} = 0^2) = \Psi_0 \geq 1$ at the origin O , this is in order to cover realistic bounded path-loss models and ensure that the received power cannot exceed the transmitted one, (ii) $\Psi(r_x; \cdot; \xi_x) \equiv \Psi(r; \cdot; \xi'_x)$ such as $r = \sqrt{r_x^2 + \xi_{x_h}^2}$ and ξ'_x is the vector $\xi'_x = (\xi_{x_t}, \xi_{x_a}, \xi_{x_b})$, (iii) the mean value of the shot noise process is finite, i.e., from the Campbell's theorem [10, Corollary 1.4.6.], we have

$$\mathbb{E} \left\{ \sum_{x \in \Phi_b} P_{rx} \right\} = \lambda_b P_{tx} \int_{\mathbb{R}^3} \frac{\mathbb{E} \{ \chi_x \} dx}{(\Psi(r_x; \alpha_x; \xi_x))^{\alpha_x}} < \infty, \quad (2)$$

The marked PPP, will be denoted, with a slight abuse of notation, also as Φ_b .

Remark 1. *The proposed model is general enough to accommodate various choices of RNPO parameters and path-loss models, e.g., if the power law path-loss is adopted and BS height is the only RNPO parameter considered [3], $\xi_x = \xi_{x_h}$ captures BSs height and $\Psi(r_x; \cdot; \xi_x) = \sqrt{r_x^2 + \xi_x^2}$. When considering also tilt angle [5], azimuth angle [6] and RE bias [7], we have $\Psi(r_x; \alpha_x; \xi_x) = \sqrt{r_x^2 + \xi_{x_h}^2} [G_{\text{tilt}}(\xi_{x_t}) G_{\text{azimut}}(\xi_{x_a}) B(\xi_{x_b})]^{\frac{1}{\alpha_x}}$, where $G_{\text{tilt}}(\cdot)$ is the antenna vertical radiation pattern parametrized by ξ_{x_t} , $G_{\text{azimut}}(\cdot)$ is the antenna horizontal radiation pattern parametrized by ξ_{x_a} and $B(\cdot)$ is the association bias parametrized by ξ_{x_b} .*

B. Path Loss process with shadowing and RNPO parameters

We define the path-loss process with shadowing and RNPO parameters (PLPSR) of Φ_b , the point process mapped from Φ_b on \mathbb{R}^+ , as

$$\Sigma = \left\{ y = \chi_x^{-1/\alpha_x} \Psi(r_x; \alpha_x; \xi_x), x \in \Phi_b \right\}. \quad (3)$$

Moreover, in order to capture the SINR threshold distribution, we consider the following independently marked PLPSR

$$\Delta = \{(\Sigma, T_x), x \in \Phi_b\}. \quad (4)$$

The following lemma gives the intensity measure of Δ , which generalizes several previous results in [11] [12].

¹We omit the dependence scenario here, e.g., ξ_x and α_x may be correlated when a tuning of the RNPO parameters ξ_x can impact α_x by determining the link nature (LOS or NLOS) between a BS and the typical user.

² $\xi_x \equiv 0$ is equivalent to no RNPO parameter considered on x , i.e., BS antenna is omnidirectional with 0 meter elevation and $B(\xi_b) \equiv 1$.

Lemma 1. *The point process Δ is a 1D independently marked PPP on \mathbb{R}^+ with intensity measure*

$$\Lambda_{\Delta}(s, t) = \frac{4\pi\lambda_b}{3} \mathbb{E} \left\{ \left[\Psi^{-1}(s\chi_x^{\frac{1}{\alpha_x}}; \alpha_x; \xi'_x) \right]^3 \mathbb{1}(T_x \leq t) \right\}, \quad (5)$$

Proof. By the displacement theorem [10, Theorem 1.3.9] and the Campbell's theorem. Δ is a PPP with intensity measure

$$\begin{aligned} \Lambda_{\Delta}(s, t) &= \lambda_b \mathbb{E} \left\{ \int_{\mathbb{R}^3} \mathbb{1} \left(\frac{\Psi(r_x; \alpha_x; \xi_x)}{\chi_x^{\frac{1}{\alpha_x}}} \leq s, T_x \leq t \right) dx \right\} \\ &\stackrel{(a)}{=} 4\pi\lambda_b \mathbb{E} \left\{ \int_{\mathbb{R}^+} \mathbb{1} \left(\frac{\Psi(r; \alpha_x; \xi'_x)}{\chi_x^{\frac{1}{\alpha_x}}} \leq s \right) \mathbb{1}(T_x \leq t) r^2 dr \right\} \\ &= \frac{4\pi\lambda_b}{3} \mathbb{E} \left\{ \int_{\mathbb{R}^+} \left[\Psi^{-1}(su^{\frac{1}{\alpha_x}}; \alpha_x; \xi'_x) \right]^3 \mathbb{1}(T_x \leq t) \mathbb{P}_{\chi_x} \{ du \} \right\} \\ &= \frac{4\pi\lambda_b}{3} \mathbb{E} \left\{ \left[\Psi^{-1}(s\chi_x^{\frac{1}{\alpha_x}}; \alpha_x; \xi'_x) \right]^3 \mathbb{1}(T_x \leq t) \right\}, \end{aligned} \quad \square$$

where (a) follows from the marks independence of the process Δ and property (ii) of $\Psi(\cdot)$.

Remark 2. *If we assume that $T_x \equiv T$ is constant over all BSs of Φ_b . It is easy to mention from lemma 1 that for the defined RNPO parameters (Remark 1), Δ is generally a homogeneous PPP with density*

$$\lambda_{\Delta}(s) = \lim_{t \rightarrow \infty} \frac{1}{4\pi s^2} \frac{\partial \Lambda_{\Delta}(s, t)}{\partial s}, \quad (6)$$

independent from s and proportionally related to $\mathbb{E} \left\{ \chi_x^{3/\alpha_x} \right\}$, e.g., when considering only height ($\xi_x \equiv \xi_{x_h}$), we have $\lambda_{\Delta} = \lambda_b \mathbb{E} \left\{ \chi_x^{3/\alpha_x} \right\} < \infty$.

Definition 1. *Similarly to [11, definition 1] and [12, definition 2], a 3D marked PPP Φ_b is said to be equivalent in distribution to a 2D marked PPP Φ'_b if they generate the same 1D marked PPP Δ with the intensity measure $\Lambda(s, t)$.*

Proposition 1. *The marked process $\Phi_b \in \mathbb{R}^3$ is stochastically equivalent to a marked PPP $\Phi'_b \in \mathbb{R}^2$ in which shadowing and RNPO parameters are not considered, i.e., $\chi'_x \equiv 1$ and $\xi'_x \equiv 0$, and endowed with marks $T'_x \equiv T_x$ whose distribution is*

$$G'_s(t) = \frac{1}{4\pi s^2 \lambda_{\Delta}(s)} \frac{\partial \Lambda_{\Delta}(s, t)}{\partial s}, \quad (7)$$

and the density of Φ'_b is expressed as $\lambda'_b(s) = 2s\lambda_{\Delta}(s)$ (8)

Proof. The proof of proposition 1 is analogous to that of [11, proposition 4]. In fact, the intensity measure of Δ' – the independently marked PLPSR of Φ'_b – when $\chi'_x \equiv 1$ and $\xi'_x \equiv 0$ is

$$\begin{aligned} \Lambda_{\Delta'}(v, t) &= 2\pi \mathbb{E} \left\{ \int_{\mathbb{R}^+} \mathbb{1}(u \leq v) \mathbb{1}(T'_x \leq t) \lambda'_b(u) u du \right\} \\ &= 2\pi \int_0^v G'_u(t) \lambda'_b(u) u du \stackrel{(a)}{=} \Lambda_{\Delta}(v, t), \end{aligned} \quad (9)$$

where (a) holds if equations (7) and (8) are met. \square

From Proposition 1, if noise, small scale fading and path-loss exponent are the same, we have then

$$\text{SINR}(x_0) = \frac{\frac{h_{x_0}\chi_{x_0}}{(\Psi(r_{x_0};\alpha_{x_0};\xi_{x_0}))^{\alpha_{x_0}}}}{\sum_{x \in \Phi_b \setminus \{x_0\}} \frac{h_x\chi_x}{(\Psi(r_x;\alpha_x;\xi_x))^{\alpha_x}} + \frac{1}{\text{SNR}}} \Big|_{\lambda_b}$$

$$\stackrel{(d)}{=} \frac{h_{y_0}y_0^{-\alpha_{y_0}}}{\sum_{y \in \Phi'_b \setminus \{y_0\}} h_y y^{-\alpha_y} + \frac{1}{\text{SNR}}} \Big|_{\lambda'_b} = \text{SINR}(y_0),$$

where $\stackrel{(d)}{=}$ denotes equivalence in distribution, $x_0 = \arg \max_{x \in \Phi_b} \{P_{\text{tx}}\chi_x (\Psi(r_x; \alpha_x; \xi_x))^{-\alpha_x}\}$ and $y_0 = \arg \max_{y \in \Phi'_b} \{y^{-\alpha_y}\}$.

III. A TRACTABLE CASE STUDY

Now, for mathematical convenience and model tractability, we take a minor detour from studying the stochastic equivalence between a 3D network with shadowing and RNPO parameters and a 2D network where they are absorbed into the model. In fact, we assume that the equivalent PPP $\Phi'_b \in \mathbb{R}^2$ is homogeneous $\lambda'_b = \lambda$, the SINR target is constant over all BSs $T'_x = T$, and the path-loss exponent α'_x is distance-dependent according to the transmission path (LOS or NLOS) between BSs and the typical user, i.e., $\alpha'_x \in \{\alpha_{\text{los}}, \alpha_{\text{nlos}}\}$ such as $\eta = \alpha_{\text{nlos}}/\alpha_{\text{los}} \geq 1$. We consider that each BS $x \in \Phi'_b$ has a LOS path towards the typical user with a LOS probability denoted P_{los} .

A. The H-LOS probability model

Since common LOS probability functions are build upon exponentially decreasing functions [13] rendering analysis less tractable, we propose to approximate them by the following piece-wise linear model, consistent with the models adopted by 3GPP [14] and dubbed here the H-LOS model,

$$P_{\text{los}}(r_x) = \begin{cases} 1 & \text{if } 0 \leq r_x \leq R_{\text{los}} \\ 1 - \frac{r_x - R_{\text{los}}}{R_{\text{nlos}} - R_{\text{los}}} & \text{if } R_{\text{los}} \leq r_x \leq R_{\text{nlos}} \\ 0 & \text{if } r_x > R_{\text{nlos}} \end{cases}, \quad (11)$$

where R_{los} is the maximum link distance between a LOS BS and the typical user such as there are no nearer NLOS BS to the typical user, while R_{nlos} is the minimum link distance between a NLOS BS and the typical user such as there are no farther LOS BS. Mathematically,

$$R_{\text{los}} = \max_{x \in \Phi_{\text{los}}} \{r_x; r_x < r_y, \forall y \in \Phi_{\text{nlos}}\}, \quad (12)$$

$$R_{\text{nlos}} = \min_{y \in \Phi_{\text{nlos}}} \{r_y; r_x < r_y, \forall x \in \Phi_{\text{los}}\}, \quad (13)$$

such as Φ_{los} and Φ_{nlos} are the PPPs of LOS and NLOS BSs of Φ'_b respectively.

Fig. 1 shows the three regions of the network generated by the H-LOS probability model in (11). Note that R_{los} and R_{nlos} can be expanded by low shadowing effect and/or RNPO actions that expand cells size (uptilt, increasing association bias, azimuth that avoid blockages...). We propose therefore the interpretation that shadowing and RNPO parameters are absorbed into the 2D PPP Φ'_b , but *their impact is still captured via the fluctuation of aggregated parameters R_{los} and R_{nlos}* .

The NLOS probability is obtained as $P_{\text{nlos}}(r_x) = 1 - P_{\text{los}}(r_x)$, $\forall x \in \Phi'_b$, and the path-loss function as

$$\mathcal{L}(r_x) = \begin{cases} r_x^{-\alpha_{\text{los}}} & \text{with probability } P_{\text{los}}(r_x) \\ K r_x^{-\alpha_{\text{nlos}}} & \text{with probability } P_{\text{nlos}}(r_x), \end{cases} \quad (14)$$

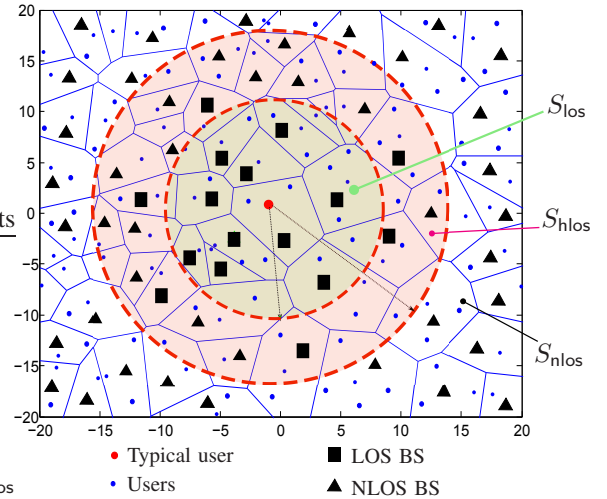


Fig. 1. S_{los} and S_{nlos} regions contain only LOS and NLOS BSs respectively, while S_{hlos} contains a mixture of the two with probability $p(r) = 1 - \frac{r - R_{\text{los}}}{R_{\text{nlos}} - R_{\text{los}}}$ for LOS BSs and $1 - p(r) = \frac{r - R_{\text{los}}}{R_{\text{nlos}} - R_{\text{los}}}$ for NLOS BSs.

where $K \triangleq R_{\text{los}}^{\alpha_{\text{los}} - \alpha_{\text{nlos}}}$ is a parameter to ensure the continuity of the path-loss function as in [9].

For positive reals m and R , we consider the following path-loss functions of interest³

$$\mathcal{L}_1(m; r_x) = r_x^{-m} \text{ and } \mathcal{L}_2(R; r_x) = \begin{cases} r_x^{-\alpha_{\text{los}}} & \text{if } r_x \leq R \\ K r_x^{-\alpha_{\text{nlos}}} & \text{if } r_x > R. \end{cases} \quad (15)$$

B. User Association Policy under the H-LOS probability model

We consider the average power-based cell association policy. Since $\eta = \alpha_{\text{nlos}}/\alpha_{\text{los}} \geq 1$ and the H-LOS probability model is adopted, the strongest BS is the nearest one in the regions S_{los} and S_{nlos} , while it is not necessarily the case in the transitional region S_{hlos} . To address this issue, we then examine the distribution of distances between the typical user and the serving BS as a result of two events: the transmission link type (LOS or NLOS), and the region to which the serving BS belongs (S_{los} , S_{nlos} or S_{hlos}). For $i \in \{\text{los}, \text{nlos}\}$, denote by S_{1i} the LOS and NLOS BSs of the S_{hlos} region respectively, by D_i the link distance from the typical user to B_i , the nearest BS of LOS and NLOS BSs respectively, and by S the serving region, i.e., the region that contains the serving BS. For BSs in Φ_i , the PDF of the horizontal distance r_x is then expressed as

$$f_{D_i}(r_x) = 2\pi\lambda r_x P_i(r_x) \exp\left(-2\pi\lambda \int_0^{r_x} u P_i(u) du\right) \quad (16)$$

Now given that $D_i = r_x$ and B_i belongs to the S_{hlos} region, it can be the serving BS if it verifies the following constraints:

$$\begin{cases} D_i^{-\alpha_{\text{los}}} > K D_{\text{nlos}}^{-\alpha_{\text{nlos}}} \Rightarrow D_{\text{nlos}} > r_0 & ; \text{ for } i = \text{los} \\ K D_i^{-\alpha_{\text{nlos}}} > D_{\text{los}}^{-\alpha_{\text{los}}} \Rightarrow D_{\text{los}} > r_1 & ; \text{ for } i = \text{nlos}, \end{cases} \quad (17)$$

where $r_0 = R_{\text{los}}^{1-\frac{1}{\eta}} r_x^{\frac{1}{\eta}}$ and $r_1 = \text{Min}(R_{\text{nlos}}, r_x^\eta / R_{\text{los}}^{\eta-1})$ holds since S_{nlos} does not contain any LOS BS.

³Note that $\mathcal{L}(\cdot) \equiv \mathcal{L}_1(\alpha_{\text{los}}; \cdot)$ when $\alpha_{\text{los}} = \alpha_{\text{nlos}}$, i.e., $R_{\text{los}} \rightarrow \infty$ or $R_{\text{nlos}} \rightarrow 0$, and $\mathcal{L}(\cdot) \equiv \mathcal{L}_2(R_{\text{los}}; \cdot)$ when $R_{\text{los}} = R_{\text{nlos}}$.

Given that $D_i = r_x$, the probability that the typical user will be connected to B_i is then given by

$$\Pi_i(r_x) = \begin{cases} 1 & \text{if } 0 \leq r_x \leq R_{\text{los}} \\ \mathbb{P}(D_{\text{nlos}} > r_0) \text{ for } i = \text{los} \\ \mathbb{P}(D_{\text{los}} > r_1) \text{ for } i = \text{nlos} & \text{if } R_{\text{los}} \leq r_x \leq R_{\text{nlos}} \\ 1 & \text{if } r_x \geq R_{\text{nlos}} \end{cases}$$

while $\mathbb{P}(D_{\text{nlos}} > r_0)$ and $\mathbb{P}(D_{\text{los}} > r_1)$ are computed using (16).

Remark 3. For $j \in \mathcal{J} = \{\text{los}, \text{1los}, \text{1nlos}, \text{nlos}\}$, The association probability $\mathcal{A}_j = \mathbb{P}(S = S_j)$ that a typical user connects to a BS from S_j , can be computed by integrating $\Pi_i(r_x) f_{D_i}(r_x)$ over each region radius interval. An interesting observation for the S_{los} region, is that for fixed parameter R_{los} , $\mathcal{A}_{\text{los}} = 1 - \exp(-\pi\lambda R_{\text{los}}^2)$ increases with λ , while the average number of users connected to S_{los} —expressed as $\widetilde{N}_{\text{los}} = (\lambda_u/\lambda)\mathcal{A}_{\text{los}}$, where λ_u is the density of the users PPP—decreases. However, for fixed λ , expanding R_{los} leads to an increase in \mathcal{A}_{los} and $\widetilde{N}_{\text{los}}$ simultaneously. More discussions are provided in Section V.

IV. COVERAGE PROBABILITY ANALYSIS

In this section, we analyze the coverage probability under our tractable system model provided in Section III, and aimed to capture the random impact of generalized shadowing and RNPO parameters via the fluctuation of aggregated parameters R_{los} and R_{nlos} .

A. Coverage Probability

We define the coverage probability under the path-loss function defined in (14), as the probability $\mathcal{P}_{\mathcal{L}}^{\text{SINR}}(\cdot)$ that the received SINR is greater than a threshold T when the serving BS belongs to one of the four sets $S_{\text{los}}, S_{\text{1los}}, S_{\text{1nlos}}$ or S_{nlos} .

Theorem 1. The coverage probability under the path-loss function (14) is given by

$$\mathcal{P}_{\mathcal{L}}^{\text{SINR}}(\cdot) = \mathcal{P}_{\text{los}}^{\text{SINR}} + \mathcal{P}_{\text{1los}}^{\text{SINR}} + \mathcal{P}_{\text{1nlos}}^{\text{SINR}} + \mathcal{P}_{\text{nlos}}^{\text{SINR}}, \quad (18)$$

where for $j \in \mathcal{J} = \{\text{los}, \text{1los}, \text{1nlos}, \text{nlos}\}$, $\mathcal{P}_j^{\text{SINR}}$ stands for the coverage probability when the serving BS belongs to S_j and the supplementary equations are listed in the top of the next page such as $a = -1/(R_{\text{nlos}} - R_{\text{los}})$, $b = -R_{\text{nlos}}/(R_{\text{nlos}} - R_{\text{los}})$, $\rho_m = (R_{\text{nlos}}/R_{\text{los}})^m$ for $m \in \mathbb{R}$, and $\delta_{p0} = p/\alpha_{\text{los}}$ and $\delta_{p1} = p/\alpha_{\text{nlos}}$ for $p = 2$ or 3 .

Proof. The sketch of the proof is as follows: The coverage probability is expressed as $\mathcal{P}_{\mathcal{L}}^{\text{SINR}}(\cdot) = \sum_{j \in \mathcal{J}} \mathcal{P}_j^{\text{SINR}}(\cdot) = \sum_{j \in \mathcal{J}} \mathcal{A}_j \mathbb{P}(\text{SINR} > T | S = S_j)$, and each component of $\mathcal{P}_{\mathcal{L}}^{\text{SINR}}(\cdot)$ will be computed with the following similar steps

$$\begin{aligned} \mathcal{P}_{\text{los}}^{\text{SINR}} &= \mathcal{A}_{\text{los}} \int_0^{R_{\text{los}}} \mathbb{P}(\text{SINR} > T | u, S = S_{\text{los}}) f_{D_{\text{los}}}(u | S = S_{\text{los}}) du \\ &\stackrel{(a)}{=} \int_0^{R_{\text{los}}} \mathbb{P}(\text{SINR}) > T | u, S_{\text{los}} \Pi_{\text{los}}(u) f_{D_{\text{los}}}(u) du \\ &\stackrel{(b)}{=} 2\pi\lambda \int_0^{R_{\text{los}}} u \exp\left(-\frac{T}{\text{SNR}} u^{\alpha_{\text{los}}} - \pi\lambda u^2\right) \mathbb{L}_{I_{S_{\text{los}} \setminus \{B_{\text{los}}\}}}(s) \mathbb{L}_{I_{S_{\text{1los}}}}(s) \\ &\quad \times \mathbb{L}_{I_{S_{\text{1nlos}}}}(s) \mathbb{L}_{I_{S_{\text{nlos}}}}(s) du, \end{aligned}$$

where $s = Tu^{\alpha_{\text{los}}}$. (a) follows from

$$f_{D_{\text{los}}}(u | S = S_{\text{los}}) = \frac{d}{du} \frac{\mathbb{P}(D_{\text{los}} \leq u, S = S_{\text{los}})}{\mathbb{P}(S = S_{\text{los}})} = \frac{\Pi_{\text{los}}(u) f_{D_{\text{los}}}(u)}{\mathcal{A}_{\text{los}}}.$$

(b) holds since $h_{B_{\text{los}}} \sim \exp(1)$ and the aggregated interference $I_{\text{agg}} = \sum_{x \in \Phi'_0 \setminus \{B_{\text{los}}\}} h_x \mathcal{L}(r_x)$ is seen as the summation of the interference power (normalized by P_{tx}) from each set $U \in \{S_{\text{los}} \setminus \{B_{\text{los}}\}, S_{\text{1los}}, S_{\text{1nlos}}, S_{\text{nlos}}\}$, i.e.,

$$\mathbb{L}_{I_{\text{agg}}}(s) = \mathbb{L}_{I_{S_{\text{los}} \setminus \{B_{\text{los}}\}}}(s) \mathbb{L}_{I_{S_{\text{1los}}}}(s) \mathbb{L}_{I_{S_{\text{1nlos}}}}(s) \mathbb{L}_{I_{S_{\text{nlos}}}}(s).$$

We get the desired result for $\mathcal{P}_{\text{los}}^{\text{SINR}}(\cdot)$ in (19) by using the PGFL theorem to compute the Laplace transforms $\mathbb{L}_{I_U}(\cdot)$ and some variable changes. \square

Remark 4. Although the expression of coverage probability under the H-LOS model is in complicated form, it instigates an intuitive algorithmic development. Moreover, the expression is general enough to accommodate several previous expressions. For example, it reflects the 3GPP case 1 study in [14] when $R_{\text{los}} \rightarrow 0$, and approximates the 3GPP case 2 study when $R_{\text{los}} \rightarrow \epsilon d_1$ and $R_{\text{nlos}} \rightarrow d_1/\epsilon$ where $0 < \epsilon < 1$ is to adjust the approximation's error. More precisely, (18) generally approximates the coverage analysis under the models in [13] by simply adjusting the parameters a and b . Furthermore, when $R_{\text{nlos}} \simeq R_{\text{los}}$, \mathcal{L} becomes a dual-slope path-loss model \mathcal{L}_2 and (18) is simplified under the expression in [3, Th. 1]. If $\alpha_{\text{nlos}} \simeq \alpha_{\text{los}}$, (18) will be the same expression as [2, Th. 2].

B. The H-LOS model and Ultra-Dense Networks

We consider the scenario of ultra-dense networks [2], where the interference I_{agg} dominates the noise normalized by the transmit power (σ^2/P_{tx}). SINR is then approximated by $\text{SIR}_{\mathcal{L}} \triangleq \text{SINR}_{\mathcal{L}} | \frac{\sigma^2}{P_{\text{tx}}} = 0$

Remark 5. In the interference-limited regime, the coverage probability in (18) remains invariant as long as λR_{los}^2 and $\lambda R_{\text{nlos}}^2$ are invariant. In other words, the impact on coverage probability of increasing/decreasing λ is analogous to increasing/decreasing $(R_{\text{los}}, R_{\text{nlos}})$ simultaneously, which is a generalization of [9, Fact 1].

In the following proposition, comparisons are made for \mathcal{P}^{SIR} under \mathcal{L}_1 , \mathcal{L}_2 and \mathcal{L} .

Proposition 2. The following SIR coverage ordering holds for arbitrary $0 < \alpha_{\text{los}} \leq \alpha_{\text{nlos}}$ and $R_{\text{los}} \leq R_{\text{nlos}}$

- (i) $\mathcal{P}_{\mathcal{L}(\cdot)}^{\text{SIR}} > \mathcal{P}_{\mathcal{L}_2(R_{\text{nlos}}; \cdot)}^{\text{SIR}} > \mathcal{P}_{\mathcal{L}_1(\alpha_{\text{los}}; \cdot)}^{\text{SIR}}$.
- (ii) $\mathcal{P}_{\mathcal{L}(\cdot)}^{\text{SIR}} < \mathcal{P}_{\mathcal{L}_2(R_{\text{los}}; \cdot)}^{\text{SIR}} < \mathcal{P}_{\mathcal{L}_1(\alpha_{\text{nlos}}; \cdot)}^{\text{SIR}}$.
- (iii) $\lim_{\lambda \rightarrow \infty} \mathcal{P}_{\mathcal{L}(\cdot)}^{\text{SINR}} = \lim_{\lambda \rightarrow \infty} \mathcal{P}_{\mathcal{L}(\cdot)}^{\text{SIR}} = \mathcal{P}_{\mathcal{L}_1(\alpha_{\text{los}}; \cdot)}^{\text{SIR}}$.
- (iv) $\lim_{\lambda \rightarrow \infty} \mathcal{P}_{\mathcal{L}(\cdot)}^{\text{SINR}} = \lim_{\lambda \rightarrow \infty} \mathcal{P}_{\mathcal{L}(\cdot)}^{\text{SIR}}(\cdot) = 0$ when $\alpha_{\text{los}} \leq 2$.
- (v) $\lim_{\lambda \rightarrow 0} \mathcal{P}_{\mathcal{L}(\cdot)}^{\text{SINR}} = \mathcal{P}_{\mathcal{L}_1(\alpha_{\text{nlos}}; \cdot)}^{\text{SIR}}$.

Proof. The proof of (i) and (ii) is similar to that of [9, Lemma 2], the main change is to proceed by considering the two cases when the serving BS $x_0 \in (S_{\text{los}} \cup S_{\text{nlos}})$ (where $\mathcal{L} \equiv \mathcal{L}_2$) and $x_0 \in S_{\text{hlos}}$. (iii) and (v) follows from the observation of Remark 5 where $\lambda \rightarrow \infty \equiv (R_{\text{los}}, R_{\text{nlos}}) \rightarrow \infty$ and $\lambda \rightarrow 0 \equiv (R_{\text{los}}, R_{\text{nlos}}) \rightarrow 0$. Such scaling in the definition of $\mathcal{L}(\cdot)$ results in $\mathcal{L}_1(\alpha_{\text{los}}; \cdot)$ or $\mathcal{L}_1(\alpha_{\text{nlos}}; \cdot)$. (iv) follows from combining (ii) and [9, Proposition 1]. While $\mathcal{P}_{\mathcal{L}(\cdot)}^{\text{SINR}} \rightarrow \mathcal{P}_{\mathcal{L}(\cdot)}^{\text{SIR}}$ as $\lambda \rightarrow \infty$ completes the proof. \square

$$\mathcal{P}_{\text{los}}^{\text{SINR}}(\text{T}) = \pi \lambda \text{R}_{\text{los}}^2 \int_0^1 \exp\left(-\frac{\text{TR}_{\text{los}}^{\alpha_{\text{los}}}}{\text{SNR}} x^{\frac{\alpha_{\text{los}}}{2}} - \pi \lambda \text{R}_{\text{los}}^2 \left[A_{\text{los}}^{(1)}(x) + \rho_2 A_{\text{los}}^{(2)}(x) + \frac{2a}{3} \text{R}_{\text{los}} A_{\text{los}}^{(3)}(x) + b A_{\text{los}}^{(4)}(x) \right]\right) dx, \quad (19)$$

$$\mathcal{P}_{1\text{los}}^{\text{SINR}}(\text{T}) = 2\pi \lambda \int_{\text{R}_{\text{los}}}^{\text{R}_{\text{nos}}} (ar^2 + br) \exp\left(-\frac{\text{T}}{\text{SNR}} r^{\alpha_{\text{los}}} - \pi \lambda \left[r_0^2 A_{1\text{los}}^{(1)}(r) + \text{R}_{\text{nos}}^2 A_{1\text{los}}^{(2)}(r) + \frac{2a}{3} A_{1\text{los}}^{(3)}(r) + b A_{1\text{los}}^{(4)}(r) \right]\right) dr, \quad (20)$$

$$\mathcal{P}_{1\text{nos}}^{\text{SINR}}(\text{T}) = 2\pi \lambda \int_{\text{R}_{\text{los}}}^{\text{R}_{\text{nos}}} ([1-b]r - ar^2) \exp\left(\frac{-\text{T}r^{\alpha_{\text{nos}}}}{K \text{SNR}} - \pi \lambda \left[r^2 A_{1\text{nos}}^{(1)}(r) + \text{R}_{\text{nos}}^2 A_{1\text{nos}}^{(2)}(r) + \frac{2a}{3} A_{1\text{nos}}^{(3)}(r) + b A_{1\text{nos}}^{(4)}(r) \right]\right) dr, \quad (21)$$

$$\mathcal{P}_{\text{nos}}^{\text{SINR}}(\text{T}) = \pi \lambda \text{R}_{\text{nos}}^2 \int_1^{\infty} \exp\left(-\frac{\text{TR}_{\text{nos}}^{\alpha_{\text{nos}}}}{\text{SNR}} x^{\frac{\alpha_{\text{nos}}}{2}} - \pi \lambda \text{R}_{\text{nos}}^2 x F_{-\delta_{21}}(\text{T})\right) dx, \quad (22)$$

$$A_{\text{los}}^{(1)}(x) = x \left[1 - F_{\delta_{20}}\left(\frac{1}{\text{T}}\right) \right] + \rho_2 F_{\delta_{21}}\left(\frac{\rho_{\alpha_{\text{nos}}}}{\text{T}x^{\delta_{20}}}\right) + \left[F_{\delta_{20}}\left(\frac{1}{\text{T}x^{\delta_{20}}}\right) - F_{\delta_{21}}\left(\frac{1}{\text{T}x^{\delta_{20}}}\right) \right], A_{\text{los}}^{(2)}(x) = F_{-\delta_{21}}\left(\frac{\text{T}}{\rho_{\alpha_{\text{nos}}}} x^{\frac{1}{\delta_{20}}}\right) - 1,$$

$$A_{\text{los}}^{(3)}(x) = \rho_3 \left[F_{\delta_{30}}\left(\frac{\rho_{\alpha_{\text{los}}}}{\text{T}x^{\delta_{20}}}\right) - F_{\delta_{31}}\left(\frac{\rho_{\alpha_{\text{nos}}}}{\text{T}x^{\delta_{20}}}\right) \right] - \left[F_{\delta_{30}}\left(\frac{1}{\text{T}x^{\delta_{20}}}\right) - F_{\delta_{31}}\left(\frac{1}{\text{T}x^{\delta_{20}}}\right) \right],$$

$$A_{\text{los}}^{(4)}(x) = \rho_2 \left[F_{\delta_{20}}\left(\frac{\rho_{\alpha_{\text{los}}}}{\text{T}x^{\delta_{20}}}\right) - F_{\delta_{21}}\left(\frac{\rho_{\alpha_{\text{nos}}}}{\text{T}x^{\delta_{20}}}\right) \right] - \left[F_{\delta_{20}}\left(\frac{1}{\text{T}x^{\delta_{20}}}\right) - F_{\delta_{21}}\left(\frac{1}{\text{T}x^{\delta_{20}}}\right) \right],$$

$$A_{1\text{los}}^{(1)}(r) = 1 - F_{\delta_{21}}\left(\frac{1}{\text{T}}\right), \quad A_{1\text{los}}^{(2)}(r) = F_{\delta_{21}}\left(\frac{\rho_{\alpha_{\text{nos}}}\text{R}_{\text{los}}^{\alpha_{\text{los}}}}{\text{T}r^{\alpha_{\text{los}}}}\right) + F_{-\delta_{21}}\left(\frac{\text{T}r^{\alpha_{\text{los}}}}{\rho_{\alpha_{\text{nos}}}\text{R}_{\text{los}}^{\alpha_{\text{los}}}}\right) - 1,$$

$$A_{1\text{los}}^{(3)}(r) = r_0^3 \left[F_{\delta_{31}}\left(\frac{1}{\text{T}}\right) - 1 \right] - r^3 \left[F_{\delta_{30}}\left(\frac{1}{\text{T}}\right) - 1 \right] + \text{R}_{\text{nos}}^3 \left[F_{\delta_{30}}\left(\frac{\text{R}_{\text{nos}}^{\alpha_{\text{los}}}}{\text{T}r^{\alpha_{\text{los}}}}\right) - F_{\delta_{31}}\left(\frac{\rho_{\alpha_{\text{nos}}}\text{R}_{\text{los}}^{\alpha_{\text{los}}}}{\text{T}r^{\alpha_{\text{los}}}}\right) \right],$$

$$A_{1\text{los}}^{(4)}(r) = r_0^2 \left[F_{\delta_{21}}\left(\frac{1}{\text{T}}\right) - 1 \right] - r^2 \left[F_{\delta_{20}}\left(\frac{1}{\text{T}}\right) - 1 \right] + \text{R}_{\text{nos}}^2 \left[F_{\delta_{20}}\left(\frac{\text{R}_{\text{nos}}^{\alpha_{\text{los}}}}{\text{T}r^{\alpha_{\text{los}}}}\right) - F_{\delta_{21}}\left(\frac{\rho_{\alpha_{\text{nos}}}\text{R}_{\text{los}}^{\alpha_{\text{los}}}}{\text{T}r^{\alpha_{\text{los}}}}\right) \right],$$

$$A_{1\text{nos}}^{(1)}(r) = 1 - F_{\delta_{21}}\left(\frac{1}{\text{T}}\right), \quad A_{1\text{nos}}^{(2)}(r) = F_{\delta_{21}}\left(\frac{\text{R}_{\text{nos}}^{\alpha_{\text{nos}}}}{\text{T}r^{\alpha_{\text{nos}}}}\right) + F_{-\delta_{21}}\left(\frac{\text{T}r^{\alpha_{\text{nos}}}}{\text{R}_{\text{nos}}^{\alpha_{\text{nos}}}}\right) - 1,$$

$$A_{1\text{nos}}^{(3)}(r) = r^3 \left[F_{\delta_{31}}\left(\frac{1}{\text{T}}\right) - 1 \right] - r_1^3 \left[F_{\delta_{30}}\left(\frac{K r_1^{\alpha_{\text{los}}}}{\text{T}r^{\alpha_{\text{nos}}}}\right) - 1 \right] + \text{R}_{\text{nos}}^3 \left[F_{\delta_{30}}\left(\frac{\rho_{\alpha_{\text{los}}}\text{R}_{\text{los}}^{\alpha_{\text{nos}}}}{\text{T}r^{\alpha_{\text{nos}}}}\right) - F_{\delta_{31}}\left(\frac{\text{R}_{\text{nos}}^{\alpha_{\text{nos}}}}{\text{T}r^{\alpha_{\text{nos}}}}\right) \right],$$

$$A_{1\text{nos}}^{(4)}(r) = r^2 \left[F_{\delta_{21}}\left(\frac{1}{\text{T}}\right) - 1 \right] - r_1^2 \left[F_{\delta_{20}}\left(\frac{K r_1^{\alpha_{\text{los}}}}{\text{T}r^{\alpha_{\text{nos}}}}\right) - 1 \right] + \text{R}_{\text{nos}}^2 \left[F_{\delta_{20}}\left(\frac{\rho_{\alpha_{\text{los}}}\text{R}_{\text{los}}^{\alpha_{\text{nos}}}}{\text{T}r^{\alpha_{\text{nos}}}}\right) - F_{\delta_{21}}\left(\frac{\text{R}_{\text{nos}}^{\alpha_{\text{nos}}}}{\text{T}r^{\alpha_{\text{nos}}}}\right) \right].$$

C. The Regime of Optimal BS Density

We define the optimal BS density $\lambda_{\mathcal{L}}^{\text{opt}}$ as the specific λ that maximizes the coverage probability under the path-loss function \mathcal{L} . Mathematically,

$$\lambda_{\mathcal{L}}^{\text{opt}}(\cdot) = \arg \lambda \left[\frac{\partial \mathcal{P}_{\mathcal{L}}^{\text{SINR}}(\cdot)}{\partial \lambda} = 0 \right]. \quad (23)$$

Using a combination of proposition 2 and [9, lemma 4], $\mathcal{P}_{\mathcal{L}}^{\text{SINR}}(\lambda)$ is a decreasing function when $\lambda > \lambda_{\mathcal{L}}^{\text{opt}}$ and $\text{SINR} \simeq \text{SIR}$. $\lambda_{\mathcal{L}}^{\text{opt}}$ can then be seen as the BS density to enter the SIR regime. We define the *optimal regime* under \mathcal{L} , the regime where the BS density $\lambda \simeq \lambda_{\mathcal{L}}^{\text{opt}}$. In this regime, the noise normalized by the transmit power is small w.r.t. the aggregated interference but it is non-zero. Consequently, (i)-(ii) of proposition 2 are at first stages to be met. We have then

$$\mathcal{P}_{\mathcal{L}_1(\alpha_{\text{los}};\cdot)}^{\text{SINR}} < \mathcal{P}_{\mathcal{L}(\cdot)}^{\text{SINR}} < \mathcal{P}_{\mathcal{L}_1(\alpha_{\text{nos}};\cdot)}^{\text{SINR}}. \quad (24)$$

$$\lambda_{\mathcal{L}_2(\text{R}_{\text{nos}};\cdot)}^{\text{opt}} < \lambda_{\mathcal{L}}^{\text{opt}} < \lambda_{\mathcal{L}_2(\text{R}_{\text{los}};\cdot)}^{\text{opt}}. \quad (25)$$

Due to the lack of general closed-form expression for $\mathcal{P}_{\mathcal{L}_1(\alpha;\cdot)}^{\text{SINR}}$ that would avoid the computation of a two-fold numerical integral in [1, theorem 1], almost all literature works focus on the Q -function based expression when the path-loss exponent $\alpha = 4$, which is only typical for terrestrial propagation at moderate to large distances. The following proposition overcome this limitation by developing closed-form expressions for

$\mathcal{P}_{\mathcal{L}_1(\alpha;\cdot)}^{\text{SINR}}$ considering all integer $\alpha > 2$ (not only $\alpha = 4$) and then conclude closed-form bounds for $\mathcal{P}_{\mathcal{L}(\cdot)}^{\text{SINR}}$ in the optimal regime.

Proposition 3. For integer path-loss exponents α_{los} and α_{nos} such as $2 < \alpha_{\text{los}} < \alpha_{\text{nos}}$. $\mathcal{P}_{\mathcal{L}}^{\text{SINR}}$ is bounded in the optimal regime as follows $\mathcal{P}_{\mathcal{L}_1(\alpha_{\text{los}};\cdot)}^{\text{SINR}} < \mathcal{P}_{\mathcal{L}(\cdot)}^{\text{SINR}} < \mathcal{P}_{\mathcal{L}_1(\alpha_{\text{nos}};\cdot)}^{\text{SINR}}$ such as the lower and upper bounds are achievable by respectively increasing R_{los} and decreasing R_{nos} , and where for even and odd values of α , respectively

$$\mathcal{P}_{\mathcal{L}_1(\alpha;\cdot)}^{\text{SINR}} = \frac{2\pi\lambda}{\alpha (\text{T}/\text{SNR})^{\frac{2}{\alpha}}} \sum_{k=0}^{\frac{\alpha}{2}-1} \frac{(-1)^k \kappa^k}{k!} \Gamma\left(\frac{2+2k}{\alpha}\right) \times {}_1F_{\frac{\alpha-2}{2}}\left(\frac{1}{\frac{4+2k}{\alpha}}, \dots, \frac{\alpha+2k}{\alpha} \mid \frac{(-\kappa)^{\frac{\alpha}{2}}}{\left(\frac{\alpha}{2}\right)^{\frac{\alpha}{2}}}\right),$$

$$\mathcal{P}_{\mathcal{L}_1(\alpha;\cdot)}^{\text{SINR}} = \frac{2\pi\lambda}{\alpha (\text{T}/\text{SNR})^{\frac{2}{\alpha}}} \sum_{k=0}^{\alpha-1} \frac{(-1)^k \kappa^k}{k!} \Gamma\left(\frac{2+2k}{\alpha}\right) \times {}_2F_{\alpha-1}\left(\frac{1, \frac{1}{2} + \frac{k+1}{\alpha}}{\frac{2+k}{\alpha}, \dots, \frac{\alpha+k}{\alpha}} \mid \frac{4(-\kappa)^{\alpha}}{\alpha^{\alpha}}\right),$$

such as $\kappa = \frac{\pi \lambda F_{-\delta}(\text{T})}{(\text{T}/\text{SNR})^{\delta}}$, $\delta = \frac{2}{\alpha}$, $\Gamma(\cdot)$ is the complete Gamma function and ${}_pF_q(\cdot)$ is the generalized hypergeometric function.

Proof. By the variable change $(\text{T}/\text{SNR})x^{\alpha/2} \rightarrow x$, the expression of $\mathcal{P}_{\mathcal{L}_1(\alpha;\cdot)}^{\text{SINR}}$ in [1, Theorem 2] can be rewritten as

$$\begin{aligned}\mathcal{P}_{\mathcal{L}_1(\alpha; \cdot)}^{\text{SINR}} &= \frac{2\pi\lambda}{\alpha(\text{T}/\text{SNR})^{\frac{\alpha}{2}}} \int_0^\infty x^{\frac{\alpha}{2}-1} e^{-x} e^{-\kappa x^{2/\alpha}} dx \\ &= \frac{2\pi\lambda}{\alpha(\text{T}/\text{SNR})^{\frac{\alpha}{2}}} \int_0^\infty x^{\frac{\alpha}{2}-1} e^{-x} {}_0F_0(\cdot; \cdot; -\kappa x^{2/\alpha}) dx.\end{aligned}$$

Depending on the parity of α , we use [15, Eq. (43)] (with $\alpha/2$ order for the even case and α order for the odd one). Next, we explore the integral transformation of hypergeometric functions in [16, (1.7.525)]. The proof is completed by combining (24) with Remark 5. \square

Using Proposition 3, the \mathcal{Q} -function based expression for $\alpha = 4$ in [1], can be rewritten for $\kappa = \pi\lambda F_{-0.5}(\text{T})\sqrt{\text{SNR}/\text{T}}$ as

$$\begin{aligned}\mathcal{P}_{\mathcal{L}_1(4; \cdot)}^{\text{SINR}} &= \frac{\pi^{\frac{3}{2}}\lambda}{2\sqrt{\text{T}/\text{SNR}}} \left[{}_0F_0\left(-; -; \left|\frac{\kappa^2}{4}\right| - \frac{\kappa}{\sqrt{\pi}} {}_1F_1\left(1; \frac{3}{2}; \left|\frac{\kappa^2}{4}\right|\right)\right) \right] \\ &= \frac{\pi^{\frac{3}{2}}\lambda}{\sqrt{\text{T}/\text{SNR}}} \mathcal{Q}\left(\frac{\kappa}{\sqrt{2}}\right) \exp\left(\frac{\kappa^2}{4}\right).\end{aligned}$$

While proposition 3 gives a complete characterization of $\mathcal{P}_{\mathcal{L}}$ in the optimal regime. The following proposition gives the scaling law of $\lambda_{\mathcal{L}}^{\text{opt}}$ as $R_{\text{los}} \rightarrow \infty$ and $R_{\text{nlos}} \rightarrow 0$.

Proposition 4. *Under the H-LOS probability model such as $2 < \alpha_{\text{los}} < \alpha_{\text{nlos}}$, the optimal BS density scales as follows*

$$(i) \lambda_{\mathcal{L}}^{\text{opt}} = \Omega\left(\left(\frac{\text{T}}{\text{SNR}}\right)^{\delta_{20}} \frac{1}{\pi F_{-\delta_{20}}(\text{T})}\right) \text{ if } R_{\text{los}} \rightarrow \infty. \quad (26)$$

$$(ii) \lambda_{\mathcal{L}}^{\text{opt}} = O\left(\left(\frac{\text{T}}{\text{SNR}}\right)^{\delta_{21}} \frac{1}{\pi F_{-\delta_{21}}(\text{T})}\right) \text{ if } R_{\text{nlos}} \rightarrow 0. \quad (27)$$

Proof. Using [9, Theorem 1], $\mathcal{P}_{\mathcal{L}_2(R_c; \cdot)}^{\text{SINR}}$ is expressed for a given radius R_c as

$$\mathcal{P}_{\mathcal{L}_2}^{\text{SINR}} = \underbrace{\lambda\pi R_c^2 \int_0^1 e^{-I_f(x) - W_f(x)} dx}_{f(\cdot)} + \underbrace{\lambda\pi R_c^2 \int_1^\infty e^{-I_g(x) - W_g(x)} dx}_{g(\cdot)},$$

$$\begin{aligned}\text{where } I_f(x) &= \lambda\pi R_c^2 \left(F_{\delta_{20}} \left(\frac{1}{\text{T}x^{\frac{1}{\delta_{20}}}} \right) + F_{-\delta_{20}} \left(\text{T}x^{\frac{1}{\delta_{20}}} \right) \right) \\ &+ \lambda\pi R_c^2 x \left(1 - F_{\delta_{20}} \left(\frac{1}{\text{T}} \right) \right) - \lambda\pi R_c^2, \quad W_f(x) = \frac{\text{T}}{\text{SNR}} R_c^{\alpha_{\text{los}}} x^{\frac{\alpha_{\text{los}}}{2}}, \\ I_g(x) &= \pi\lambda R_c^2 x F_{-\delta_{21}}(\text{T}) \text{ and } W_g(x) = \frac{\text{T}}{\text{SNR}} R_c^{\alpha_{\text{los}}} x^{\frac{\alpha_{\text{nlos}}}{2}}.\end{aligned}$$

We note that I_f and I_g are the terms reflecting interference while W_f and W_g are those capturing noise. In the optimal regime under \mathcal{L}_2 , i.e., $\lambda \simeq \lambda_{\mathcal{L}_2(R_c; \cdot)}^{\text{opt}}$, W_f and W_g are respectively negligible w.r.t. I_f and I_g but non zero. We expand then the terms $e^{-W_f(x)}$ and $e^{-W_g(x)}$ as $e^{-\mu} = \sum_{k=0}^n \frac{(-\mu)^k}{k!} + E_n(\mu)$, where E_n is the error of approximation such as $E_n(\mu) \leq \frac{|\mu|^{n+1}}{(n+1)!}$ [17]. The error of approximation of $\mathcal{P}_{\mathcal{L}_2}^{\text{SINR}}$ in the optimal regime is then upper bounded as

$$|E_n| \leq \lambda\pi R_c^2 A^{n+1} U_n + \lambda\pi R_c^2 B^{n+1} V_n, \text{ where} \quad (28)$$

$$A \simeq \frac{\text{T}}{(\lambda\pi R_c^2 F_{-\delta_{20}}(\text{T}))^{\frac{\alpha_{\text{los}}}{2}} \text{SNR}}, \quad B = \frac{\text{T} R_c^{\alpha_{\text{los}}}}{(\lambda\pi R_c^2 F_{-\delta_{21}}(\text{T}))^{\frac{\alpha_{\text{nlos}}}{2}} \text{SNR}},$$

$$U_n = \frac{\gamma((n+1)\frac{\alpha_{\text{los}}}{2} + 1, \pi\lambda R_c^2 F_{-\delta_{20}}(\text{T}))}{(n+1)!}, \text{ and}$$

$$V_n = \frac{\Gamma((n+1)\frac{\alpha_{\text{nlos}}}{2} + 1, \pi\lambda R_c^2 F_{-\delta_{21}}(\text{T}))}{(n+1)!},$$

where $\gamma(s, x) = \int_0^x t^{s-1} e^{-t} dt$ and $\Gamma(s, x) = \int_x^\infty t^{s-1} e^{-t} dt$ are the lower and upper incomplete gamma function.

For any given error tolerance ϵ , the bound (28) gives

$$A \leq \left(\frac{\epsilon}{\lambda\pi R_c^2 2U_n}\right)^{\frac{1}{n+1}}, \quad B \leq \left(\frac{\epsilon}{\lambda\pi R_c^2 2V_n}\right)^{\frac{1}{n+1}}. \quad (29)$$

If $R_c \rightarrow \infty$ and since $\alpha_{\text{los}} > 2$, $U_n \rightarrow \infty$ as $n \rightarrow \infty$ and then $\left(\frac{\epsilon}{\lambda\pi R_c^2 2U_n}\right)^{\frac{1}{n+1}} \rightarrow 1$ as $n \rightarrow \infty$. (29).1 simplifies as

$$\lambda \geq \left(\frac{\text{T}}{\text{SNR}}\right)^{\delta_{20}} \frac{1}{\pi F_{-\delta_{20}}(\text{T})}, \quad (30)$$

$$\Rightarrow \exists \omega_f \geq 1 \text{ such as } \lambda_{\mathcal{L}_2(R_c; \cdot)}^{\text{opt}} = \left(\frac{\text{T}}{\text{SNR}}\right)^{\delta_{20}} \frac{\omega_f}{\pi F_{-\delta_{20}}(\text{T})}. \quad (31)$$

If $R_c \rightarrow 0$ and since $\alpha_{\text{nlos}} > 2$, $V_n \rightarrow \infty$ as $n \rightarrow \infty$ and then $\left(\frac{\epsilon}{\lambda\pi R_c^2 2V_n}\right)^{\frac{1}{n+1}} \rightarrow 1$ as $n \rightarrow \infty$. (29).2 simplifies as

$$\lambda \geq \left(\frac{\text{T}}{\text{SNR}}\right)^{\delta_{21}} \frac{1}{\pi F_{-\delta_{21}}(\text{T})}, \quad (32)$$

$$\Rightarrow \exists \omega_g \geq 1 \text{ such as } \lambda_{\mathcal{L}_2(R_c; \cdot)}^{\text{opt}} = \left(\frac{\text{T}}{\text{SNR}}\right)^{\delta_{21}} \frac{\omega_g}{\pi F_{-\delta_{21}}(\text{T})}. \quad (33)$$

The proof is completed by combining (31) and (33) with (25). \square

Remark 6. *By varying one parameter and fixing the others in (26) and (27), $\lambda_{\mathcal{L}}^{\text{opt}}$ is monotonically increasing with the SINR target T , the noise variance σ^2 and the path-loss exponents, while it is decreasing with the transmit power P_{tx} (intuitively, the higher you increase P_{tx} the less you will need more BSs). Besides, $\lambda_{\mathcal{L}}^{\text{opt}}$ cannot be increased indefinitely with T . In fact, for a real $0 < m < 1$, $\psi_m : \text{T} \rightarrow \text{T}^m / F_{-m}(\text{T})$ is an increasing function bounded as $\psi_m(\text{T}) \leq \lim_{\text{T} \rightarrow \infty} \psi_m(\text{T}) = \frac{1}{\varphi(m)}$, where $\varphi(m) = \int_0^\infty \frac{du}{1+u^m}$ is finite (Riemann integral).*

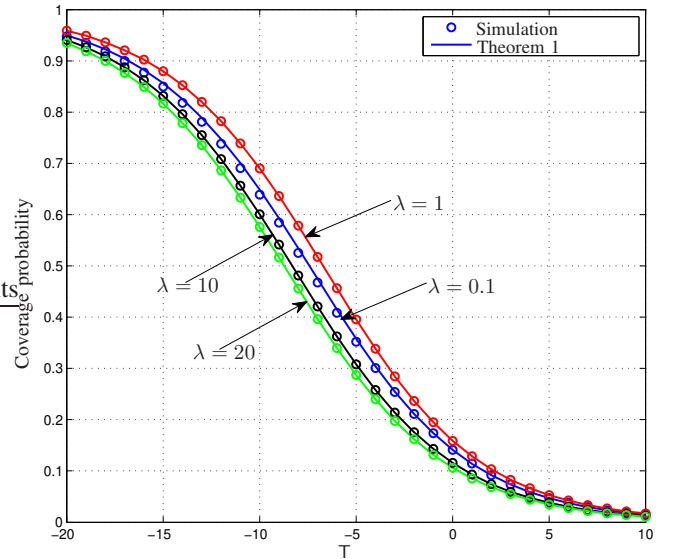


Fig. 2. Coverage probability from both Theorem 1 and simulation results. $\alpha_{\text{los}} = 2$, $\alpha_{\text{nlos}} = 4$, $R_{\text{los}} = 1\text{m}$ and $R_{\text{nlos}} = 10\text{m}$.

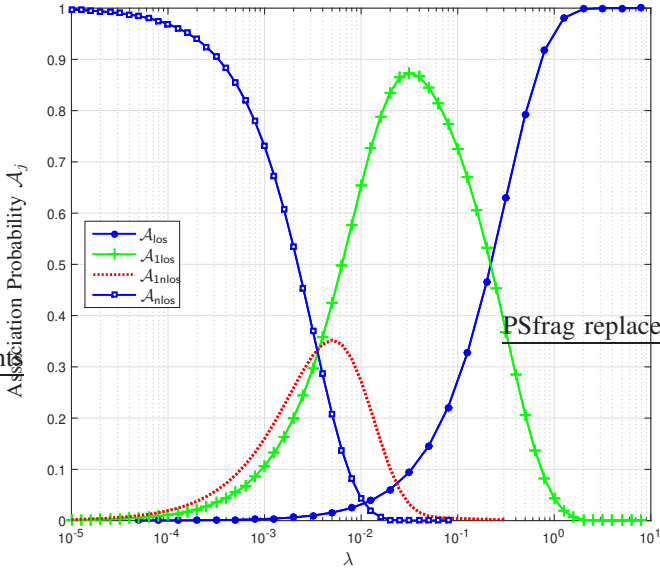


Fig. 3. Association probability scaling with BS density λ for $R_{\text{los}} = 1\text{m}$ and $R_{\text{nlos}} = 10\text{m}$.

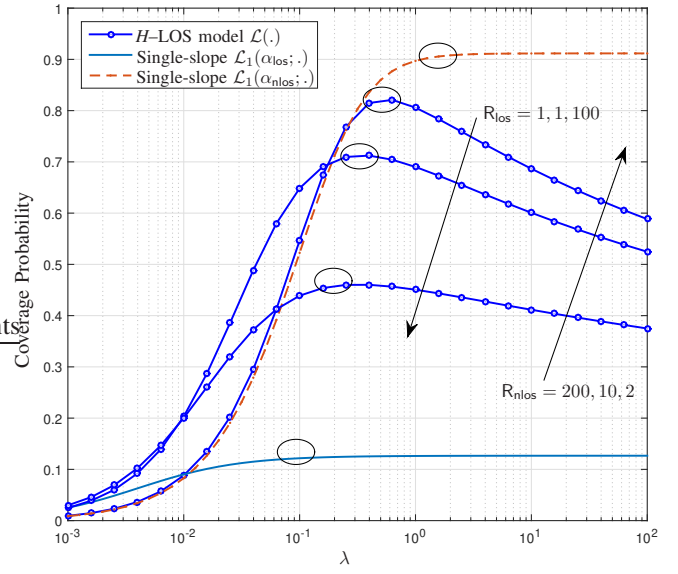


Fig. 5. Scaling of $\lambda_{\mathcal{L}}^{\text{opt}}$ with R_{los} and R_{nlos} variations, $\alpha_{\text{los}} = 2.03$, $\alpha_{\text{nlos}} = 4$ and $T = -10\text{dB}$.

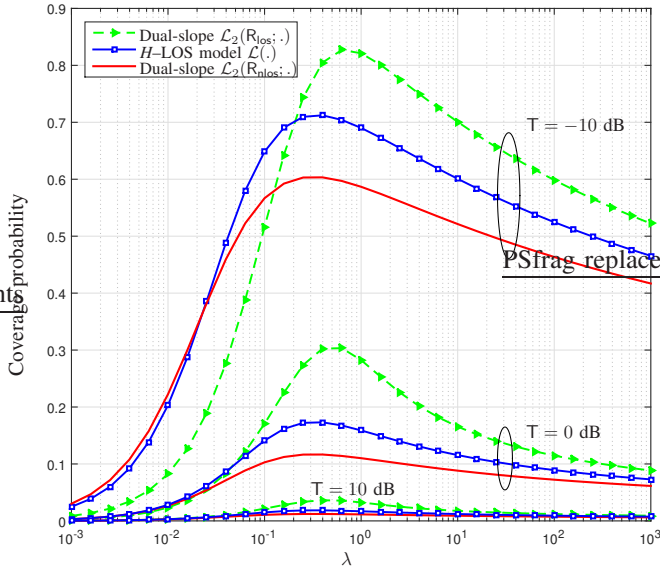


Fig. 4. Coverage probability scaling with λ under \mathcal{L} and \mathcal{L}_2 path-loss models, $R_{\text{los}} = 1\text{m}$ and $R_{\text{nlos}} = 10\text{m}$, $\alpha_{\text{los}} = 2$ and $\alpha_{\text{nlos}} = 4$.

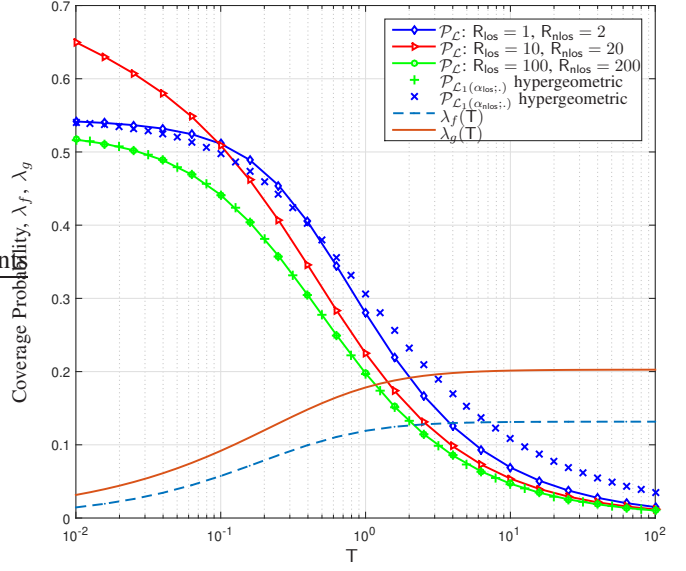


Fig. 6. Coverage probability scaling with network density λ for \mathcal{L} and \mathcal{L}_2 path-loss models. $R_{\text{los}} = 1\text{m}$ and $R_{\text{nlos}} = 10\text{m}$ and path-loss exponents $\alpha_{\text{los}} = 2$ and $\alpha_{\text{nlos}} = 4$.

V. NUMERICAL RESULTS AND DISCUSSIONS

In this section, we present numerical results to assess our theoretical analysis. In the following, $\text{SNR} = 0\text{dB}$, integral expressions are evaluated using Matlab and Monte carlo simulations are performed with 10^6 iterations.

A. Validation of the model

The expression of coverage probability in (18) configured with path-loss exponents $\alpha_{\text{los}} = 2$, $\alpha_{\text{nlos}} = 4$ and a given realization of BSs, shadowing and RNPO parameters such as $R_{\text{los}} = 1\text{m}$ and $R_{\text{nlos}} = 10\text{m}$, is plotted in Fig. 2. The

plots show that the analytical expression match the simulation results well, and hence the accuracy of our theoretical analysis is validated. In particular, Fig. 2 shows that the coverage probability increases at first with network density λ until achieving the optimal value $\lambda_{\mathcal{L}}^{\text{opt}}$, after that $\mathcal{P}_{\mathcal{L}}^{\text{SINR}}$ shrinks down as densification continue.

B. The Association probabilities and operational regimes

A combination of Fig. 3 and Fig. 4, reveals that when $\lambda < 0.0035\text{BSs/m}^2$, the serving BS is potentially to be a BS from the S_{nlos} set and the operational regime is the noise-limited

regime where $I_{\text{agg}} \ll (\sigma^2/P_{\text{tx}})$; this is due to the observation that the network will be more sparse and the inter-distance between BSs is high enough such that I_{agg} can be ignored. As λ slightly increases ($\lambda \rightarrow 0.0035$ BSs/m²), the typical user is more likely to connect unsteadily to an NLOS BS from the hybrid region S_{hlos} . By continuously adding more BSs (0.0035 BSs/m² $< \lambda < 0.2$ BSs/m²), the serving BS crosses to be a LOS BS from S_{hlos} . Once λ is large enough ($\lambda > 0.2$ BSs/m²), the typical user is most likely to connect to a BS from S_{los} and thus the coverage probability continues to increase until λ achieves a specific value $\lambda_{\mathcal{L}}^{\text{opt}} \simeq 0.4$ BSs/m². At that level, $\mathcal{P}_{\mathcal{L}_3}^{\text{SIR}}$ achieves its maximum value and follows the regression driven by interference I_{agg} as λ continue to increase.

C. Coverage Probability and BS Density Scaling in The Optimal Regime

Fig. 4 and Fig. 5 verifies Proposition 2 in the optimal regime as the coverage probability $\mathcal{P}_{\mathcal{L}}^{\text{SINR}}$ and the optimal BS density $\lambda_{\mathcal{L}}^{\text{opt}}$ remain bounded between those achieved under the standard and dual-slope path-loss functions. Numerically, $0.12 < \mathcal{P}_{\mathcal{L}}^{\text{SINR}} < 0.9$ and 0.1 BSs/m² $< \lambda_{\mathcal{L}}^{\text{opt}} < 1$ BSs/m². In particular, the lower and upper bounds are achievable for sufficient expansion and shrinking on R_{los} and R_{nlos} respectively.

Fig. 6 is consistent with Proposition 3 and 4. In fact, for the purpose to assess the accuracy of $\mathcal{P}_{\mathcal{L}}$ bounds approximation in the optimal regime, we limit first the scaling of $\mathcal{P}_{\mathcal{L}}$ with T into this regime by considering the combinations ($\lambda = \lambda_g$; $R_{\text{los}} = 1$; $R_{\text{nlos}} = 2$), ($\lambda = \frac{\lambda_f + \lambda_g}{2}$; $R_{\text{los}} = 10$; $R_{\text{nlos}} = 20$) and ($\lambda = \lambda_f$; $R_{\text{los}} = 100$; $R_{\text{nlos}} = 200$), where $\lambda_f = \frac{T^{\delta_{20}}}{\pi F^{-\delta_{20}}(T)}$ and $\lambda_g = \frac{T^{\delta_{21}}}{\pi F^{-\delta_{21}}(T)}$. As can be observed from Fig. 6 for $\alpha_{\text{los}} = 3$ and $\alpha_{\text{nlos}} = 4$, λ_f and λ_g are increasing with the SINR target T until a stage where they become stable and independent from T (Remark 6). Moreover, $\mathcal{P}_{\mathcal{L}}^{\text{SINR}}$ remains bounded by the hypergeometric closed-form expression of $\mathcal{P}_{\mathcal{L}_1}^{\text{SINR}}(\alpha_{\text{los}}; T)$ for $\lambda = \lambda_f$ and $\mathcal{P}_{\mathcal{L}_1}^{\text{SINR}}(\alpha_{\text{nlos}}; T)$ for $\lambda = \lambda_g$.

VI. CONCLUSION

In this paper, we investigated the importance of introducing generalized shadowing and conventional RNPO parameters into the cell-selection model. Using tools from SG, we established an SINR distribution equivalence between a 3D network with shadowing and RNPO parameters and a 2D network in which they are ignored.

Next, for mathematical convenience and model tractability, we proposed an equivalent 2D network based on the H-LOS probability model such as the effect of shadowing and RNPO parameters is interpreted as captured via the fluctuation of aggregated parameters R_{los} and R_{nlos} . We derived then the coverage probability and confirmed that its formulation generalizes that of several previous works. Moreover, the regimes where coverage probability is maximized as well

as the interference-limited one are investigated based on the scaling of R_{los} and R_{nlos} , which implicitly reflects different realization of shadowing and RNPO parameters. An intermediary result is a generalisation of the special case closed-form expression in [1]. Our results give practical insights for operators and vendors considering the deployment of ultra-dense 5G networks.

REFERENCES

- [1] J. G. Andrews, F. Baccelli, and R. K. Ganti, "A tractable approach to coverage and rate in cellular networks," *IEEE Trans. Commun.*, vol. 59, no. 11, pp. 3122-3134, Nov. 2011.
- [2] N. Bhushan et al., "Network densification: The dominant theme for wireless evolution into 5G," *IEEE Commun. Mag.*, vol. 52, no. 2, pp. 82-89, Feb. 2014.
- [3] I. Atzeni, J. Arnau, and M. Kountouris, "Downlink cellular network analysis with LOS/NLOS propagation and elevated base stations," *IEEE Trans. Wireless Commun.*, vol. 17, no. 1, pp. 142-156, Jan. 2018.
- [4] A. Merwaday, R. Vannithamby, M. M. Rashid, Y. Zhang, C. Chen, and X. Wu, "Tilt angle optimization in two-tier cellular networks – A stochastic geometry approach," *IEEE Trans. Commun.*, vol. 63, no. 12, pp. 5162-5177, Dec. 2015.
- [5] R. Hernandez-Aquino, S. A. R. Zaidi, D. McLernon, M. Ghogho, and A. Imran, "Tilt angle optimization in two-tier cellular networks – A stochastic geometry approach," *IEEE Trans. Commun.*, vol. 63, no. 12, pp. 5162-5177, Dec. 2015.
- [6] B. Blaszczyzyn, and M. K. Karray, "Spatial distribution of the SINR in Poisson cellular networks with sector antennas," *IEEE Trans. Wireless Commun.*, vol. 15, no. 1, pp. 581-593, Jan. 2016.
- [7] H. S. Jo, Y. J. Sang, P. Xia, and J. G. Andrews, "Heterogeneous cellular networks with flexible cell association: A comprehensive downlink SINR analysis," *IEEE Trans. Wireless Commun.*, vol. 11, no. 10, pp. 3484-3495, Oct. 2012.
- [8] J. G. Andrews, X. Zhang, G. D. Durgin, and A. K. Gupta, "Are we approaching the fundamental limits of wireless network densification?" *IEEE Commun. Mag.*, vol. 54, no. 10, pp. 184-190, Oct. 2016.
- [9] X. Zhang, and J. G. Andrews, "Downlink cellular network analysis with multi-slope path loss models," *IEEE Trans. Commun.*, vol. 63, no. 5, pp. 1881-1894, May 2015.
- [10] F. Baccelli, and B. Blaszczyzyn, "Stochastic Geometry and Wireless Networks: Volume I theory," *Found. Trends Netw.*, vol. 4, nos. 3-4, pp. 249-449, 2010.
- [11] B. Blaszczyzyn, and H. P. Keeler, "Equivalence and comparison of heterogeneous cellular networks," in *Proc. IEEE 24th Annu. Symp. Pers. Indoor Mobile Radio Commun. Workshops (PIMRC)*, London, U.K., 2013, pp. 153-157.
- [12] P. Madhusudhanan, J. Restrepo, Y. Liu, T. Brown, and K. Baker, "Downlink performance analysis for a generalized shotgun cellular system," *IEEE Trans. Wireless Commun.*, vol. 13, no. 12, pp. 6684-6696, Dec. 2014.
- [13] S. Sun, T. A. Thomas, T. S. Rappaport, H. Nguyen, I. Z. Kovacs, and I. Rodriguez, "Path loss, shadow fading, and line-of-sight probability models for 5G urban macro-cellular scenarios," in *Proc. IEEE Glob. Conf. Workshops (GLOBECOM)*, San Diego, CA, USA, 2015, pp. 1-7.
- [14] M. Ding, P. Wang, D. Lopez-Perez, G. Mao, and Z. Lin, "Performance impact of LoS and NLoS transmissions in dense cellular networks," *IEEE Trans. Wireless Commun.*, vol. 15, no. 3, pp. 2365-2380, Mar. 2016.
- [15] A. P. Prundnikov, Y. A. Brychkov, and O. I. Marichev, *Integrals and Series, Vol. 3: More Special Functions*, Philadelphia, USA: Gordon and Breach Science Publishers, 1990.
- [16] I. S. Gradshteyn, I. M. Ryzhik, *Table of Integrals, Series, and Products*, 7th ed. Academic Press, Elsevier Inc, 2007.
- [17] S. Guruacharya, H. Tabassum and E. Hossain, "Integral approximations for coverage probability," *IEEE Wireless Commun. Letters*, vol. 5, no. 1, pp. 24-27, Feb. 2016.